LASER INTERFEROMETER GRAVITATIONAL WAVE OBSERVATORY
- LIGO -
CALIFORNIA INSTITUTE OF TECHNOLOGY
MASSACHUSETTS INSTITUTE OF TECHNOLOGY

Technical Note	**LIGO-T1500194–vX**	2015/10/04

Feedforward Seismic Noise Cancellation at the 40m Interferometer

Jessica Pena
Mentors: Eric Quintero, Koji Arai, Rana Adhikari

California Institute of Technology
LIGO Project, MS 18-34
Pasadena, CA 91125
Phone (626) 395-2129
Fax (626) 304-9834
E-mail: info@ligo.caltech.edu

Massachusetts Institute of Technology
LIGO Project, Room NW22-295
Cambridge, MA 02139
Phone (617) 253-4824
Fax (617) 253-7014
E-mail: info@ligo.mit.edu

LIGO Hanford Observatory
Route 10, Mile Marker 2
Richland, WA 99352
Phone (509) 372-8106
Fax (509) 372-8137
E-mail: info@ligo.caltech.edu

LIGO Livingston Observatory
19100 LIGO Lane
Livingston, LA 70754
Phone (225) 686-3100
Fax (225) 686-7189
E-mail: info@ligo.caltech.edu

http://www.ligo.caltech.edu/

Abstract

The interferometers used by LIGO (Laser Interferometer Gravitational Wave Observatory) are subject to a multitude of noise sources. These noise sources, if not properly accounted for, will eliminate the possibility of gravitational wave detection. Seismic noise and the self-noise of devices used are two main noise sources that can be filtered out using a variety of physical and mathematical filters. The goal of this project was to develop mathematical filters to reduce self-noise of our seismometers and accelerometers, both of which are used to measure seismic noise. I used both FIR and IIR Wiener filters, in combination with pre-filtering, to account for these noise sources. The main pre-filter explored was an elliptic bandpass filter, focusing on a region of lower frequencies, where we expect the instruments? self-noise interferes most with the interferometer signal. Combining such a pre-filter with a Wiener filtered out a significant amount of instrument self-noise.

Contents

1 Background

1.1 Noise in LIGO Interferometers

LIGO Interferometers send a laser beam through a beam splitter to be locked in Fabry-Perot cavities and recombined so that the effects of the environment in the cavity can be observed [1]. Gravitational waves are ideally detected by observing effects of the wave on the laser. However, many other factors aside from gravitational waves affect the resulting signal from the lasers. These outside factors are noise that must be filtered out either through the construction of a mathematical filter or physically building a filter to dampen the noise. Many kinds of noise affect LIGO Interferometers, but Seismic noise and instrumental self-noise are currently some of the most problematic because they affect frequencies LIGO is trying to detect and are more difficult to precisely control mechanically [1]. Mechanical filters, including stabilizing the concave mirrors in each cavity through magnetic fields and using oscillators to dampen seismic noise, are already in place but are always being improved.

1.2 Feedforward vs Feedback Filtering

Mathematical filters are just as important as physical filters. Mathematical filters can be feedback or feedforward. Feedforward techniques must precisely predict what the seismic noise will look like and then adjust the detector so that this particular noise is not part of the output. Feedback adjusts the detector after noise has propagated through the system [2]. The differences between feedforward and feedback are depicted below (figure 1). In a

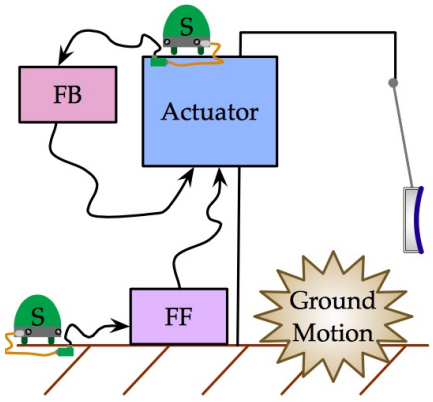

Figure 1: The differences between a feedback loop and a feedforward loop [3]

feedback loop, the disturbances and noise sources must pass through the system in order to be detected, whereas with feedforward these noise sources are predicted and preemptively filtered out. Thus, there is no time lag in feedforward filters as is present in feedback filters [2]. Wiener filters in particular are desirable to use for feedforward techniques because they determine the value of an unknown signal given known signals while minimizing the RMS of the error. Using feedback, one can determine the noise of the system and then construct a feedforward Wiener filter based off of that [3]. These filters will have an extensive impact,

minimizing seismic noise through multiple degrees of freedom [4]. Therefore, we will only need to construct one Wiener filter to filter out noise from several sources.

1.3 Difference Between IIR and FIR Wiener Filters

In this case, IIR Wiener filters are ideal because they require fewer parameters than FIR filters, which is important because Wiener filters have to create a very precise model of the system, so the fewer parameters required means that there is less room for error. This also drastically reduces computational time of the filters by using IIR instead of FIR coefficients [4]. This is especially important for a feedforward system, which must predict how to filter the signal prior to receiving it. Also, IIR filters are more likely to achieve the lowest mean-square error because they are computed by integral, while a FIR filter is a summation [5]. Therefore, FIR filters can come close to achieving the results of IIR filters, but will never be quite as good. However, IIR filters are difficult to calculate, and they also can introduce noise into controls of the system because of how each control interacts with others [4]. Therefore, it will be difficult to implement an IIR filter that also optimizes subtraction and introduces minimal noise into other parts of the system.

1.4 The 40m Prototype Interferometer Setup

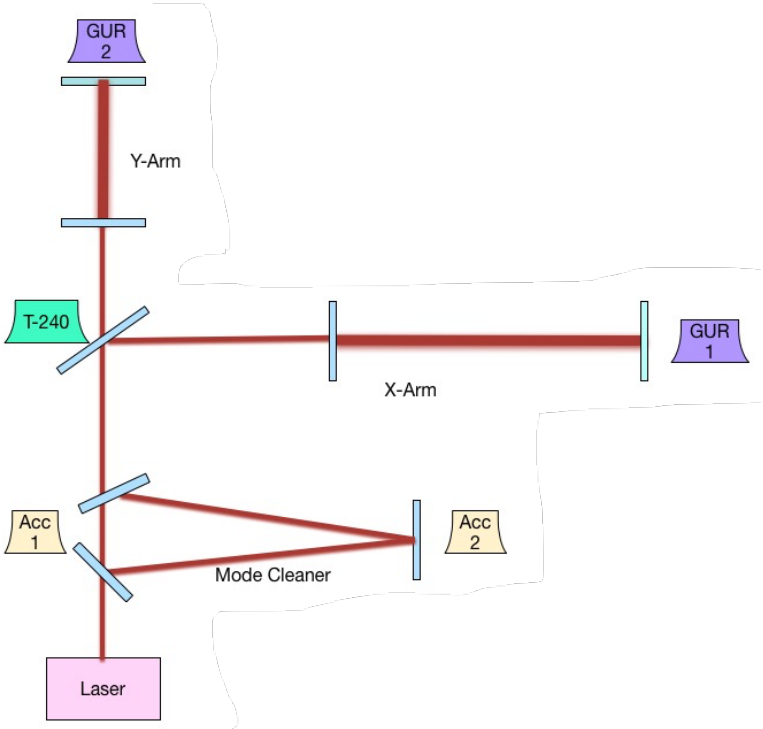

Figure 2: The layout of the 40m Lab

At the 40m Prototype Interferometer, I will be applying a feedforward online IIR Wiener filter to the mode cleaner length. As can be seen in figure 2, the laser travels through the mode cleaner before entering the arms. The mode cleaner helps stabilize the laser. There is

an accelerometer at each end of the mode cleaner, each having an X, Y, and Z component. There are also three seismometers, a Trillium-240 seismometer located at the beam splitter, and a Guralp seismometer located at the end of each arm. All the seismometers have three channels. Using the accelerometers and seismometers, I will be able to accurately model and predict seismic noise. A Wiener filter can then filter out seismic noise from the mode cleaner, helping to further stabilize the laser before it enters the arms. Therefore, filtering noise out of the mode cleaner potentially will also remove noise from the arms, making the mode cleaner an ideal target.

2 Goals for the Summer

2.1 Weeks 1-4

During the first several weeks of the summer, I compared various algorithms and techniques of filtering noise from our sensors to determine self-noise. Self-noise is important to know because it cannot be mechanically be filtered out and gives us a maximum subtraction goal. We use both seismometers and piezoelectric accelerometers to detect seismic noise, so it is important to know the self-noise of both. Piezoelectric accelerometers are solid state devices, consisting of a crystal and a seismic mass. When a force is applied to the crystal by seismic motion, a voltage is created across it which we then measure.[6]. A seismometer consists of a weight on a spring, with the attached frame connected to the earth's surface. Seismometers act as a transducer between the input acceleration and the position of the mass [7]. They also behave similarly to accelerometers at small frequencies. In either case, we can measure the input and output of individual sensors, but have no way to physically isolate the noise from a single sensor. As a result, we must use multiple sensors, which all measure the same signal, and then use the differences in these results to determine the noise in an individual sensor. I applied the Three-Cornered Hat Technique and Wiener filtering to accelerometers which we had performed a huddle test on. Wiener filtering was applied to seismometers.

2.2 Weeks 5-10

After analyzing data using the Three-Cornered Hat Technique and FIR (Finite Impulse Response) Wiener filters, I explored other options for noise reduction. While the first two methods did filter out a significant amount of noise, the filtered noise curve was still significantly higher than the predicted self-noise of the accelerometers. Pre-filtering the data and then applying a Wiener filter is one way to further reduce data. Pre-filtering is important because, if excess noise can be removed before running the data through a filter, the filter will be more accurate and a greater overall reduction of noise will occur [8]. This month, I focused on researching various forms of pre-filtering and ultimately used an elliptic bandpass filter. I also explored the IIR (Infinite Impulse Response) Wiener filter as another offline alternative to the FIR Wiener filter. The IIR filter will also be easier to implement in an online subtraction. After implementing on offline IIR Wiener filter, my goal was to create an online IIR Wiener filter. To do this, I first had to fit the actuator to MCL transfer function using vectfit. Using this, I then had to construct an IIR Wiener filter and extract zeros, poles, and the gain as coefficients to put into the online system. I also looked into

more methodical ways to pre-filter, and ran through different parameters in an attempt to optimize the pre-filter.

3 Three-Cornered Hat Method

3.1 Three-Cornered Hat Technique

The Three-Cornered Hat Method is an algorithm to determine the error of one measurement of a given quantity after multiple measurements were taken. This is useful when, experimentally, we have no way to measure the quantity in a control environment, but must always deal with noise. As accelerometers will always detect vibrations, this method is useful to determine the self-noise of a single accelerometer. The propagation of uncertainty, or how the uncertainty of a variable x affects the uncertainty of f(x), is integral to understanding the Three-Cornered Hat Technique. Allan and Gray explain this method by having a single variable "x" of unknown quantity and then taking three measurements of it [9].

$$u1 = x \pm e1 \qquad u2 = x \pm e2 \qquad u3 = x \pm e3 \tag{1}$$

The only information we can directly measure are the three quantities u1, u2, and u3 in equation (1). From there however, we can calculate the variations between these measurements: σ_{12}^2, σ_{13}^2, and σ_{23}^2. We also know that the sigmas add linearly such that

$$\sigma_{12}^2 = \sigma_1^2 + \sigma_2^2 \tag{2}$$

$$\sigma_{13}^2 = \sigma_1^2 + \sigma_3^2 \tag{3}$$

$$\sigma_{23}^2 = \sigma_2^2 + \sigma_3^2 \tag{4}$$

We can then obtain the expression for σ_1^2 by combining equation (2), (3), and (4):

$$\sigma_1^2 = \frac{1}{2}(\sigma_{12}^2 + \sigma_{13}^2 - \sigma_{23}^2) \tag{5}$$

[9]. We have now obtained a sigma for just one signal, successfully extracting the noise for one measurement by analyzing the differences between three observed quantities.

To apply this method to data taken from accelerometers and seismometers, the PSD (Power Spectral Density) must be taken of the differences between the signals. The variance (σ) shown in equations (2) - (5) becomes the PSD of the difference between the two signals. As PSDs are how the signal from accelerometers and seismometers are generally viewed and compared, it makes sense that the variance would be a PSD. In turn, these lead to the PSD being plotted and compared before and after the Three-Cornered Hat method was applied.

3.2 Three-Cornered Hat Results

I used the Three-Cornered Hat method to determine the noise in accelerometers subject to the huddle test. To perform a huddle test, the six accelerometers were grouped together so that each measures the same quantity. They were also clamped to the table to reduce

differences in seismic noise between them. Given the results of the huddle test, I was able to calculate the Power Spectral Density (PSD) for each accelerometer and determine its self-noise using the Three-Cornered Hat technique. Following the steps outlined in Section 3, I made the plots in two sets of three, determining the noise of accelerometers 1-3 separately from accelerometers 4-6. Figure 3 shows the noise levels for the first three accelerometers using the Three-Cornered Hat method. It can be seen here that at lower frequencies, espe-

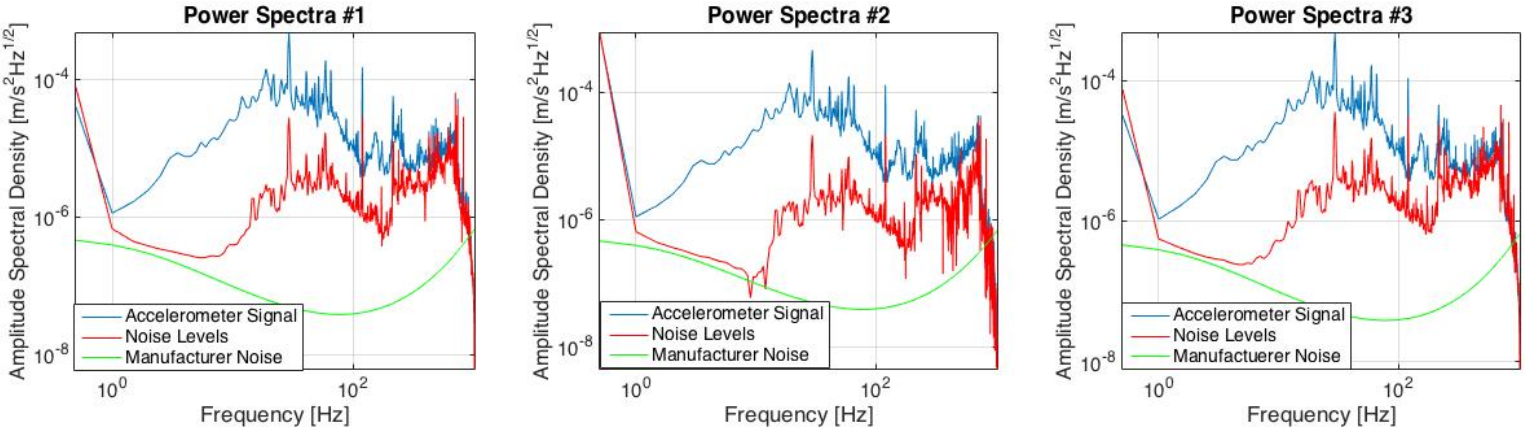

Figure 3: PSD plots for the noise in the first three accelerometers in the huddle test, made by the Three-Cornered Hat method

cially between 1 and 10 Hz, the Amplitude Spectral Density (ASD) has been significantly lowered, while at higher frequencies the Three-Cornered Hat method did not filter as much out. Comparing this to the expected noise, which is the green line, it can be seen that what has been filtered out by the Three-Cornered Hat method is still significantly higher than is desired between 10 and 1000 Hz.

4 FIR Wiener Filtering

4.1 Constructing a Wiener Filter

MISO (Multiple Input Single Output) Wiener filters are used to calculate noise by comparing multiple input signals to an output signal. This is useful in determining the self-noise of accelerometers and seismometers, and has the potential to filter out seismic noise better than the Three-Cornered Hat method can. As can be seen in figure 4, an input signal coming from a seismometer or accelerometer is run through a Wiener filter. From here, we can compare the output $y(n)$ to the predicted, or desired, signal $d(n)$. This produces an error signal which is used to determine how well the Wiener filter worked. Describing the error signal as

$$e(n) = d(n) - \vec{w}x(n) \tag{6}$$

emphasizes the difference between the desired signal and the measured signal [10]. The Wiener filter, described here by $\vec{w}$, is a vector of coefficients that are applied to the input signal to produce the output signal that is to be minimized. The coefficients of a Wiener

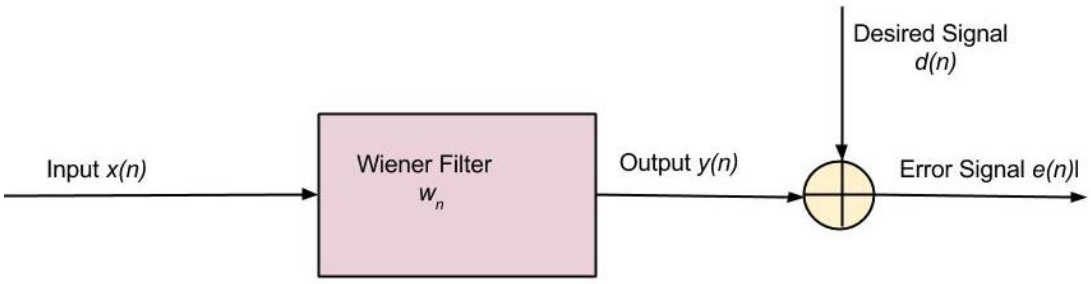

Figure 4: Wiener Filter

filter come from solving this RMS minimization equation:

$$\xi =< d^2 > -2\vec{\omega}^T\vec{p} + \vec{\omega}^T R\vec{\omega} \tag{7}$$

where ξ is what we will minimize to calculate the Wiener coefficients, d is the signal we wish to filter, $\vec{\omega}$ is the Wiener filter we are solving for, $\vec{p}$ is the cross-correlation vector between witness and target signals described by

$$\vec{p} =< x(n) * d(n) > \tag{8}$$

and R is the cross-correlation matrix describing the correlation between each input signal with the others[10]. This matrix is given by

$$R\vec{w} = \vec{p} \tag{9}$$

which means that the matrix R must be inverted for the Wiener coefficients in $\vec{w}$ to be extracted. Given an array of vector sources and a vector output, the Wiener filter determines coefficients that can be applied to the input data to remove noise from it. The Block-Levinson method was used to calculate a SISO (Single Input Single Output) filter, while a brute force method for matrix inversion was used when calculating MISO Wiener filters.

4.2 MISO Filtering of Accelerometers

I first created a MISO Wiener filter and applied it to the accelerometer data from the huddle test. This way, I can later compare the Three-Cornered Hat method of determining self-noise to the ability of the Wiener filter to do the same. To create a Wiener filter for these accelerometers, I used a Matlab function that implemented the matrix algebra described in the section above. Each accelerometer was a separate input. There was no specific output. Instead, I used 2 accelerometers as input and a third as output to determine the self-noise of the "output" accelerometer. The results of this (figure 5) were successful. Comparing the Wiener filter of the accelerometers to the Three-Cornered Hat method of determining self-noise of accelerometers, as is pictured below (figure 6), I found that the Wiener filter worked much better, especially taking high frequencies into account. In low frequency ranges both methods produce similar results, but the significantly lower noise curve at high frequencies produced by the Wiener filter is promising. It motivates further exploration into the Wiener filter, including adaptive as opposed to static filters. A combination of Wiener filtering and the Three-Cornered Hat method also holds potential to filter noise down to the manufacturer's predicted level.

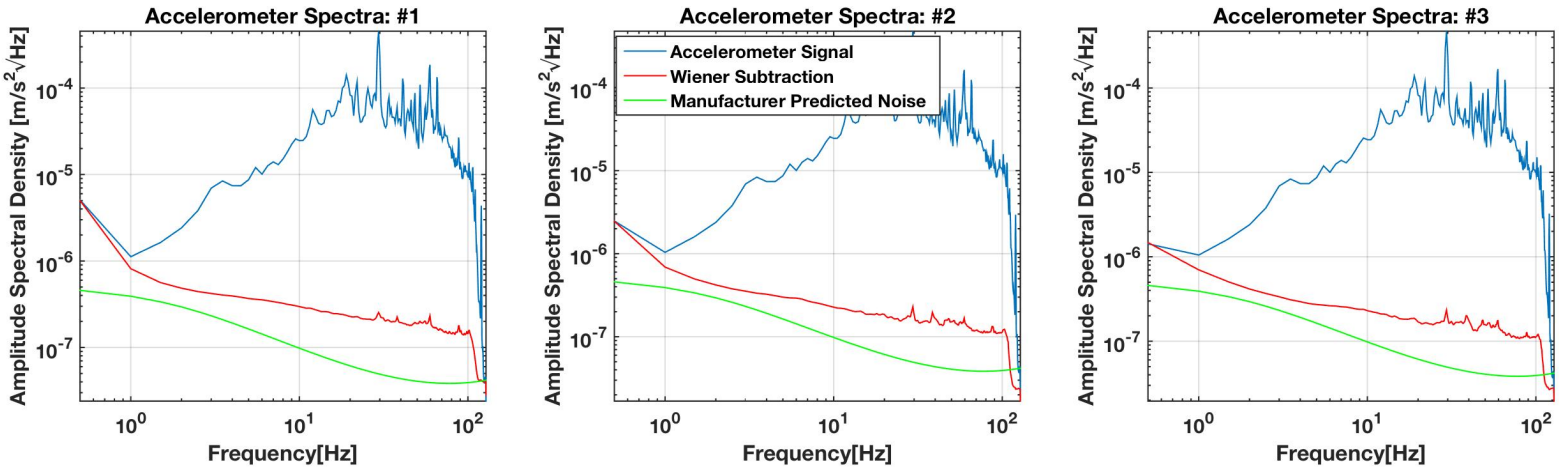

Figure 5: MISO Wiener filtering of the first three accelerometers in the huddle test

4.3 MISO Filtering of All Sensors

I then used Matlab to apply MISO filtering to a seismometer having components in the x, y, and z directions along with the two accelerometers at the end of each arm (figure 2). The seismometer was measuring noise around the mode cleaner, so all three components had an output corresponding to the mode cleaner. The two accelerometers also each had three directional components. I used the accelerometers and seismometers to find one set of Wiener coefficients. Subtracting all of this from the output and then finding the PSD resulted in the plot below (figure 7). This filter successfully reduced noise in the 3-10 Hz range.

5 Pre-Filtering

5.1 Methods

Pre-filtering data will improve the subtraction of the Wiener filter by emphasizing certain frequencies more than others. As the goal of pre-filtering is to reduce the RMS of the error signal, it will improve the Wiener filter, which is designed with the same goal in mind. Typical pre-filters include Butterworth, Chebyshev I, Chebyshev II, and Elliptic filters. These in turn can be bandpass, lowpass, or high-pass filters. Lowpass filters remove high frequencies while high-pass filters filter out lower frequencies. Bandpass filters allow a certain range of frequencies through to be emphasized, which is why this is the ideal filter for the mode cleaner length, which has noise both above and below the frequencies of interest. Once the filter type is chosen, there are specific parameters of the filter that must be specified. Passband ripple and stop-band attenuation are two of these parameters that determine how well the filter works. As can be seen in figure 8, the passband ripple is the amount of variation allowed in the passband, or the region containing allowed frequencies. The stop-band attenuation allows for fluctuation in the region of blocked frequencies [13]. A lower passband ripple and higher stop-band attenuation has proved to work best in the data I have filtered so far. Each filter results in a transfer function of varying complexity. Butterworth filters are the simplest

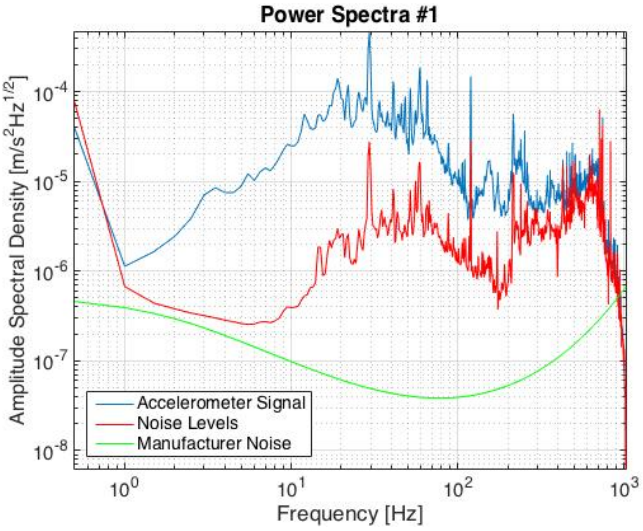

(a) Three Cornered Hat method applied to the first accelerometer in the huddle test

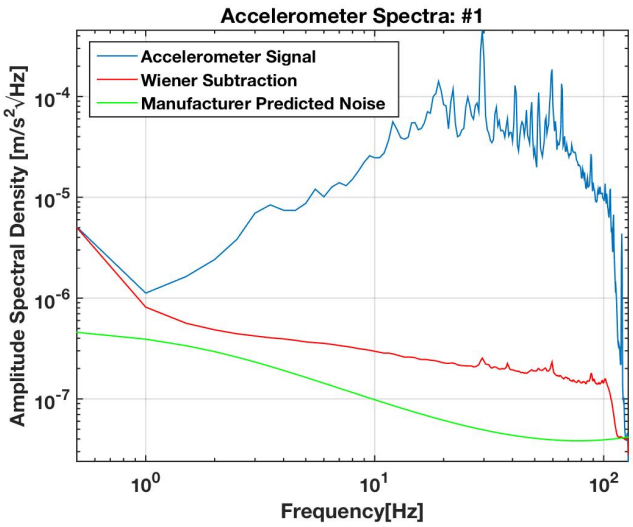

(b) MISO Wiener filtering of the first accelerometer in the huddle test

Figure 6: Comparison between the Three-Cornered hat method (a) and MISO filtering (b)

filters, with a transfer function H(s) [11] of

$$H(s)H(-s) = 1 + (-s^2)^n \tag{10}$$

This will result in a maximally flat passband, and is also simple enough that passband ripple and stop-band attenuation are not taken into account. This transfer function, while simple, also means that the transition between the passband and stop-band is very slow, so there will be no sharp drop as is depicted in figure 8, but there will instead be a slope and excess noise from the stop-band will be allowed through the filter [11]. Both Chebyshev filters are more precise than the Butterworth filter. Chebyshev I filters allow for passband ripple only, while Chebyshev II filters only allow ripple in the stop-band [12]. This makes each of them more precise and complex than Butterworth filters. Elliptic filters are the most complex filter, allowing both passband ripple and stop-band attenuation. This transfer function is much more complex [11]

$$H(jw)^2 = 1 + [\epsilon R_n(\frac{w}{w_B}, L)]^2 \tag{11}$$

By accounting for passband ripple and stop-band attenuation, elliptic filters are most precise and will calculate a filter with a very low order that has the same result as a high ordered Butterworth filter [11]. This makes elliptic filters computationally ideal, as Matlab will be able to calculate a low-ordered elliptic filter much faster than a high ordered Butterworth filter. With decreased run-time, implementing an online pre-filter will become much more plausible.

5.2 Pre-Filtering of Mode Cleaner Length Data

To reduce noise in the data for the mode cleaner length, I implemented a third order elliptic bandpass filter in Matlab. I focused on frequencies between 1 and 20 Hz. These frequencies

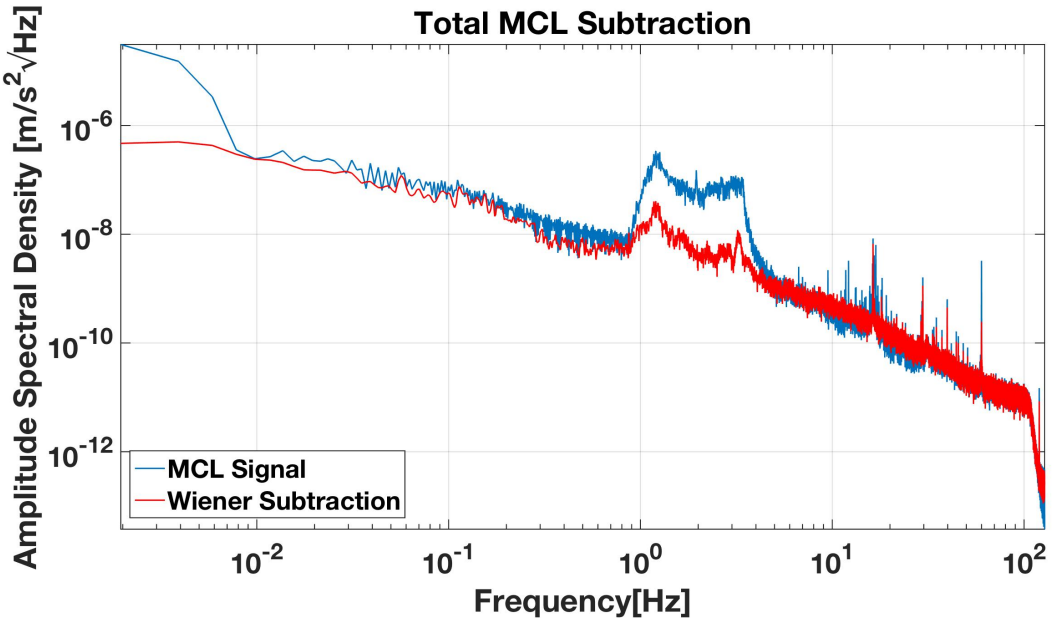

Figure 7: Filtering noise in seismometer and 2 accelerometers out of mode cleaner

encompass the range that we want to focus on, so noise reduction is most important in this range. So far, the results from this filter are a minimal improvement from Wiener filtering alone. Figure 9 illustrates this, and that noise is injected in ranges outside of 1-20 Hz. However, since there are no excessive noise injections outside this range, meaning that the excess noise never rises far above the original signal, the filter is still good to have. To calculate this filter, I used a passband ripple of 1 dB and a stop band attenuation of 20 dB. I also looked into designing a pre-filter more methodically. To do this, I used filters of increasing complexity and ran over parameters. To start, I designed a Butterworth filter and looped through 10 different filter orders. By plotting the RMS after each iteration, I was able to see that the improvement of the RMS quickly became minimal as the filter order increased. Therefore, I chose a lower degree filter. Continuing in a similar manner with the Chebyshev I, Chebyshev II, and Elliptic filters, I was able to construct a pre-filter that should be ideal. However, as can be seen in Figure 9, this pre-filter did not do much. It is probable that adjusting each parameter separately will not work as well as if I had adjusted several at once, taking into account how changing one can affect the others.

6 IIR Wiener Filtering

6.1 IIR Wiener Filtering Using Vectfit

Once a working pre-filter has been calculated for the mode cleaner length, the pre-filtered data is run through vectfit to create an IIR (Infinite Impulse Response) Wiener filter. Similar inputs and outputs to the ones described in section 5 are used in IIR Wiener filters. However, the transfer function must first be calculated for each input before data can be interpreted by vectfit. Once the transfer function is calculated, zpk coefficients can be calculated by

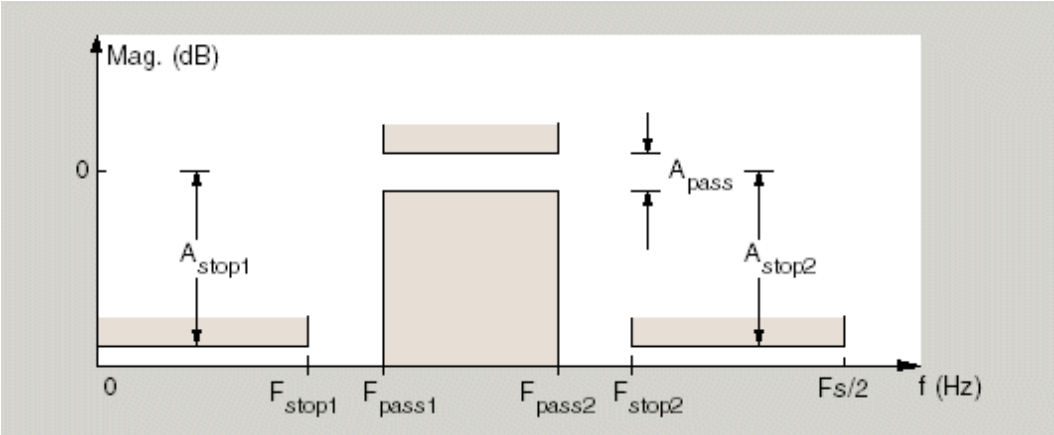

Figure 8: Image of stop-band attenuation and passband ripple [13]

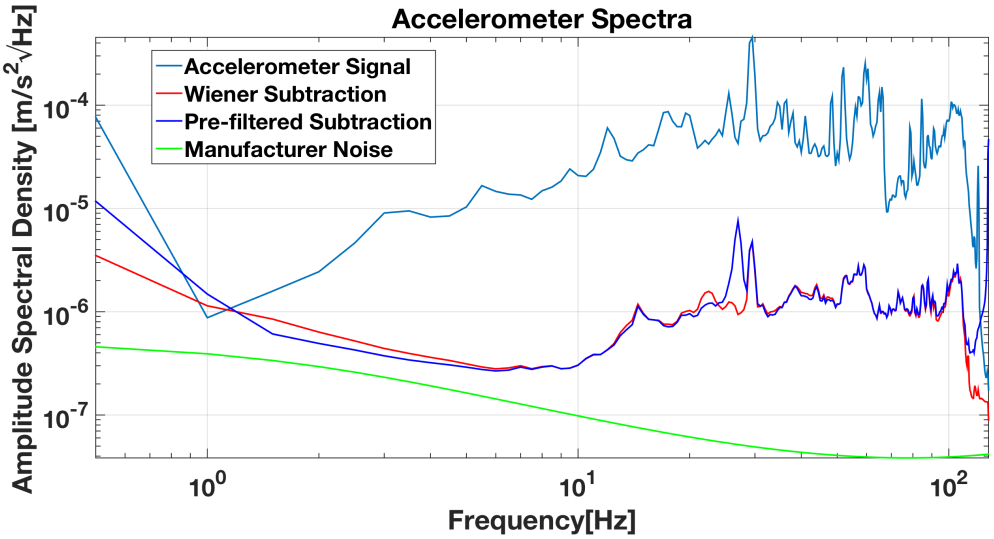

Figure 9: The use of a pre-filter (dark blue) did not improve subtraction much

solving the following equation:

$$\sigma(s) = \frac{\Pi(s - z_m)}{\Pi(s - a_m)} \tag{12}$$

From here, zeros, poles, and gain can be obtained by the Matlab code for vectfit [14].It is also important to pre-weight the data before it is used by vectfit. Pre-weighting emphasizes one region of frequencies, allowing one region to be minimized the most by the subtraction. Vectfit take the transfer function and finds the zeros, poles, and gain (zpk) of the function [14]. As vectfit returns the zpk coefficients in the s-domain, I then transform these to the z-domain. From there, a second-order section model is created, which can then be applied to the data and filter it appropriately. Choosing a small yet effective number of zeros and poles, in combination with pre-weighting, is the most difficult part of IIR Wiener filtering.

6.2 Results of offline IIR Wiener Filtering

Using an IIR Wiener filter has made little difference from using a FIR Wiener filter. It is probable that the pre-weighting factor used needs to be optimized. In Figure 10, the pre-weighting for the IIR Wiener filter was $1/\sqrt{tf}$, where tf is the transfer function. This is an improvement from no pre-weighting, but designing a pre-weight to optimize the area between 1 and 20 Hz is the next step in this process. Online IIR subtraction will be implemented in the coming week, with the hopes that it will lower the noise. As the current settings have not increased noise levels and did as well as FIR Wiener subtraction, it is the hope that IIR online subtraction will work just as well.

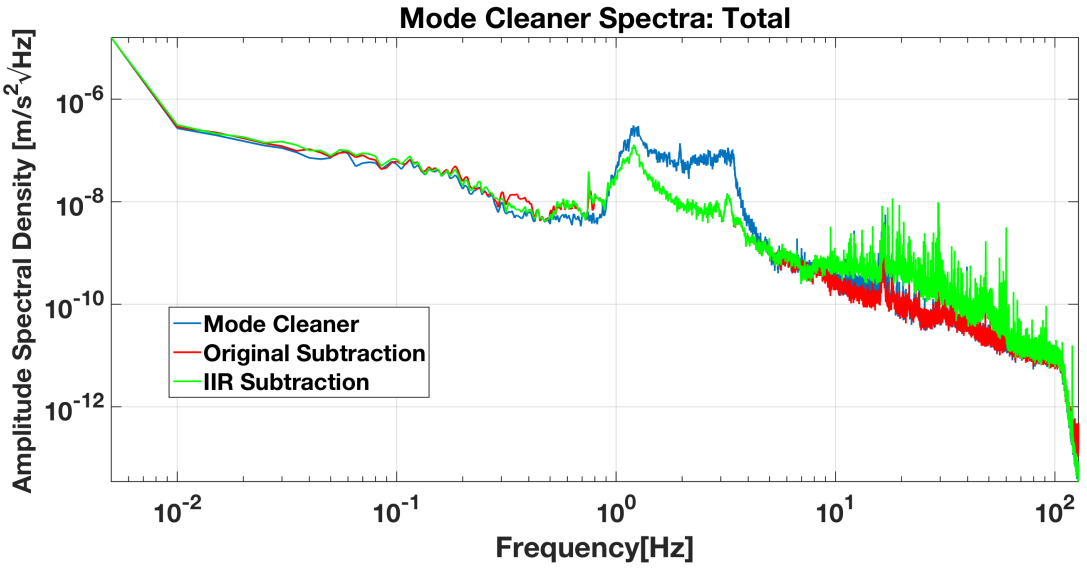

Figure 10: Comparison of FIR vs. IIR Wiener Filtering of accelerometer self-noise out of the mode cleaner length

6.3 Online IIR Wiener Filtering

Once offline IIR Wiener Filtering has been achieved, online IIR Wiener filtering is the next goal. Online filtering occurs in real time and changes the position of the mirror by adjusting the actuator which controls the mirror. As can be seen in figure 11, the ground motion goes into both the PEM sensors and the Mechanical Plant. The PEM sensors are the accelerometers and seismometers. From there, the measured but otherwise untouched signal travels through the Wiener filter, and then to the actuator which adjusts the mirror, and lastly through to the mode cleaner. The 'H' placed before the Wiener filter is the measured transfer function of the actuator to the mode cleaner length. This was measured separately, and then used as a pre-filter to the IIR Wiener filter. Applying this transfer function is one of the big differences of online as opposed to offline filtering. However, the transfer function also had to be fit and zpk coefficients had to be extracted for it using vectfit. This means that, to do online IIR Wiener subtraction, two different vectfits are required, which leaves a lot of room for error and the fits potentially not being good enough to reduce subtraction.

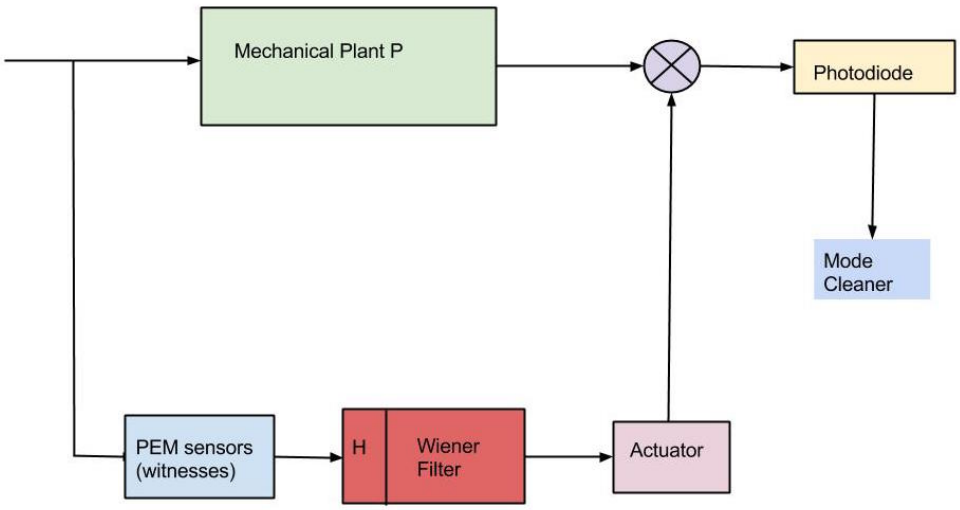

Figure 11: Diagram of implementing Online Feedforward Wiener Filtering

6.4 Online IIR Wiener Filtering Results

Testing the online IIR Wiener filter gave less ideal results than offline subtraction for the most part. It can be seen that, in the Mode Cleaner Length, there was subtraction and also no noise injection. Noise injection can be a problem with online subtraction, even more so than with offline subtraction, because online subtraction actually moves the mirrors. Therefore, bad noise injection can unlock the mode cleaner or one of the arms. In the Y-Arm, there is

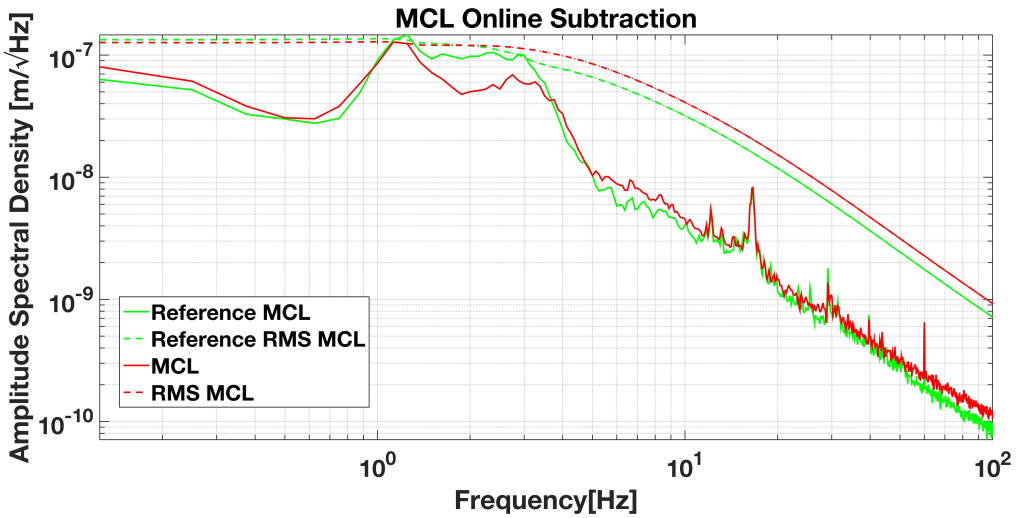

Figure 12: Online Mode Cleaner Length Subtraction

even less subtraction than in the Mode Cleaner Length. We would expect to see subtraction here when filtering the mode cleaner because the mode cleaner functions as a pre-filter for the laser before it enters the arms. Therefore, reducing noise in the mode cleaner should also lead to a cleaner signal in the arms. This also means that there is potential for the

online filter to inject noise into the arms. As can be seen in the Y-Arm, there was a slight reduction in noise, but also a noticeable noise injection at 40-70 Hz. This limits the current setup, and finding a way to improve the fit for the transfer function could potentially remove this injection. When comparing online and offline subtractions directly (figure 14), it can be

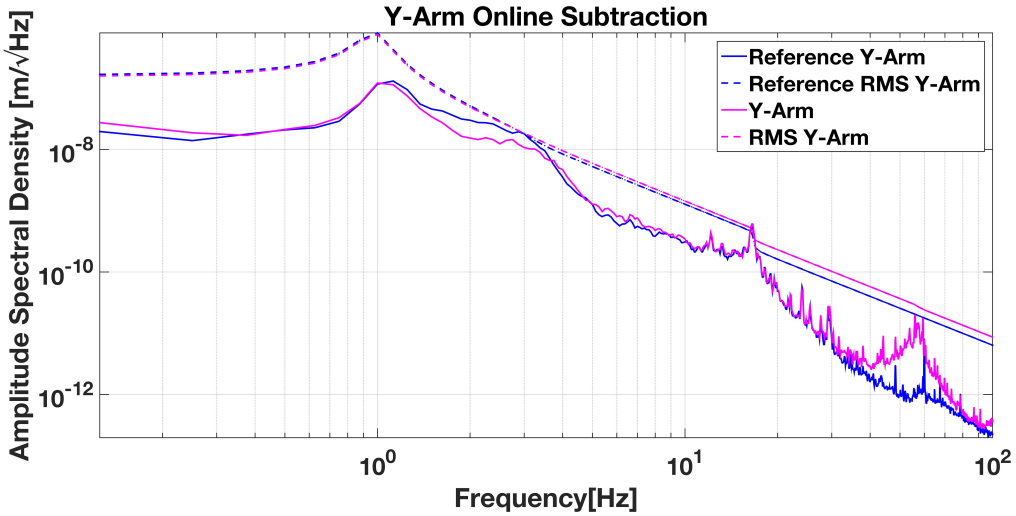

Figure 13: Online Y Arm Subtraction

seen the offline FIR subtraction currently works best. However, FIR is very computationally expensive, so IIR Wiener filters are still preferred. The offline IIR is significantly better than the online subtraction. However, better vectfitting of both the transfer function and the IIR fit itself can help increase the subtraction of the online IIR Wiener Filter.

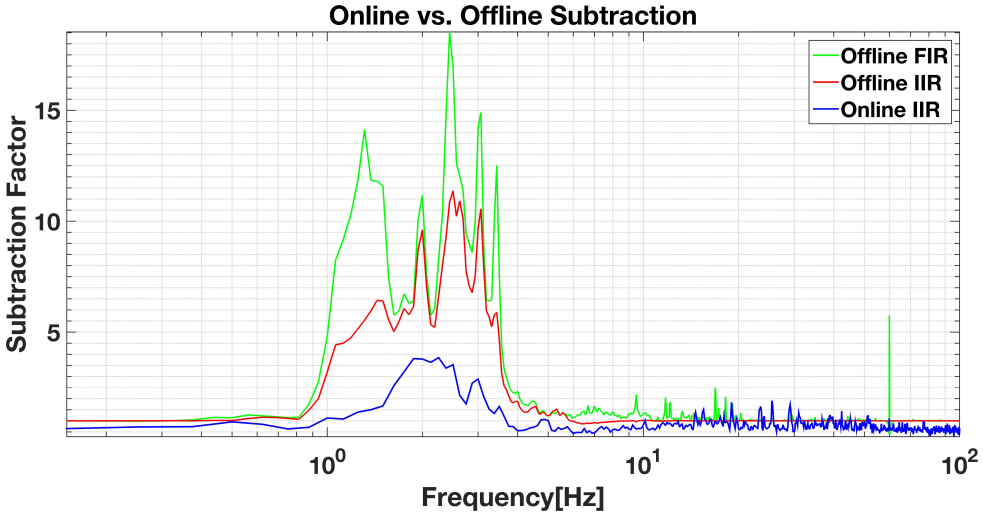

Figure 14: Subtraction offline vs. online

7 Future Research

Both pre-filtering and online Wiener filtering are ongoing processes. Pre-filtering can be done in a more methodical manner. While I have been working on this, I think that being able to know how to optimize multiple parameters at once would be helpful. Optimizing each individually ignores how they interact with each other or if there is a better balance between them. Online Wiener filtering has many directions to be explored further. Better fitting of the transfer function and the IIR Wiener filter itself is one of them. Finding a way to eliminate noise injection in the Y-Arm is also extremely important if online filtering is to be effective.

8 Appendix

8.1 Arm Length Stabilization Delay Line Time Delay

While working on a Wiener filter, I also worked on another project trying to physically isolate the 50m long ALS (Arm Length Stabilization) Delay line cables. My goal was to keep the cables seismically and electrically isolated. To do this, I had to put them inside the same conductive box so that they feel the same seismic vibrations while being inside a Faraday cage to keep them electrically isolated. When the cables arrived, I had to determine the time delay in the cables. To do this, I created Bode plots for each cable. I then wrote a code in Matlab that found the time delay in each cable by finding the slope of the phase [rad] versus the frequency [Hz]. Both cables had a time delay of 127 ns.

8.2 ALS Delay Line Box Front Panel Testing

When the front panels for the delay line box arrived, I was able to build the ALS Delay Line box. I divided it with a conductive grid of metal to prevent crosstalk between the two cables. I also covered both cables with foam to prevent them from moving around too much. Once the box was constructed, I tested both the front panels with conductive and isolated SMAs to determine if crosstalk was occurring between the cables. I did this by driving a frequency through one of the cables, and driving another frequency less than 800 Hz different from the first through the second cable. Looking at the PSDs of these should reveal if crosstalk occurs, as if it does, spikes will be visible at the frequency of the difference between the driving frequencies.

8.3 ALS Delay Line Analysis

For the conductive SMA panel, I drove 29.537 MHz through the X Arm and 29.5372 MHz through the Y Arm, giving a difference of 200 Hz. The X Arm PSD is shown in figure 15a and the Y Arm PSD is shown in figure 15b. Three sets of data are shown in each plot. The first set was taken when frequencies were being driven through both cables, while the next two were when one of the cables had a frequency driven through it and the other was off. I centered each plot around 200 Hz, because if crosstalk was occurring then a spike would appear when a frequency was driven through both cables but not when one cable was off. So, in both the Y Arm and X Arm data, a spike can be seen at 200 Hz when both cables were on but not when just one was. This indicates that crosstalk may be going on when the conductive SMAs are used.

However, data from the isolated SMA panel shows similar results to the conductive panel. Driving 29.537 MHz through the X Arm and 29.5372 MHz through the Y Arm, there was a difference of 200 Hz between the cables in the isolated front panel. Similarly to the data for the conductive front panel, it can be seen in figures 16a and 16b that there is a spike at 200 Hz, which is exactly the difference between the frequencies driven through the arms. This spike indicates potential crosstalk between the cables. However, the spikes with the isolated panel were smaller than the crosstalk spikes using the isolated panel. However, as there was still a clear spike present with both panels in the test setup, both panels would have to be

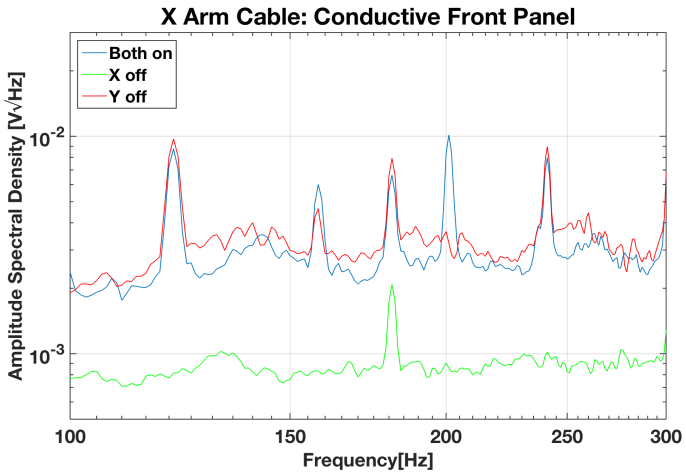

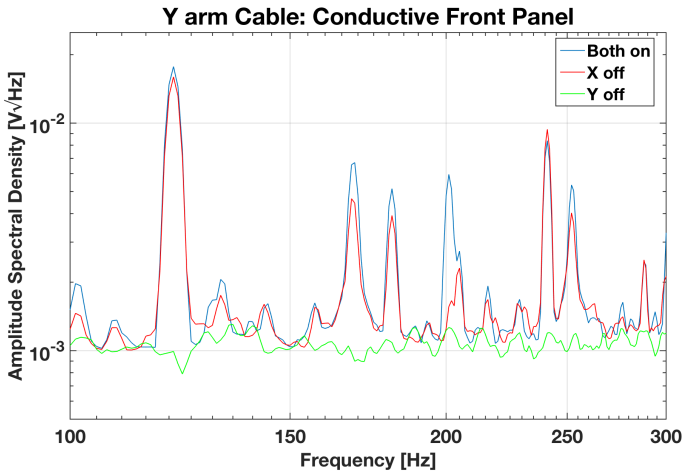

(a) X arm cable data using conductive front panel (b) X arm cable data using isolated front panel

Figure 15: Comparison between conductive X (a) and the conductive Y(b)

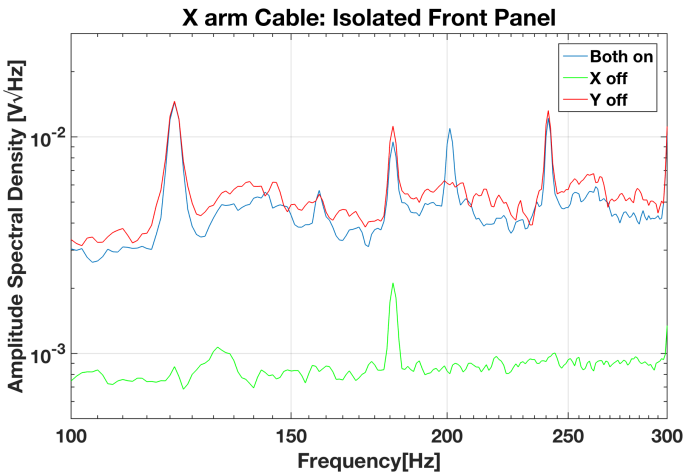

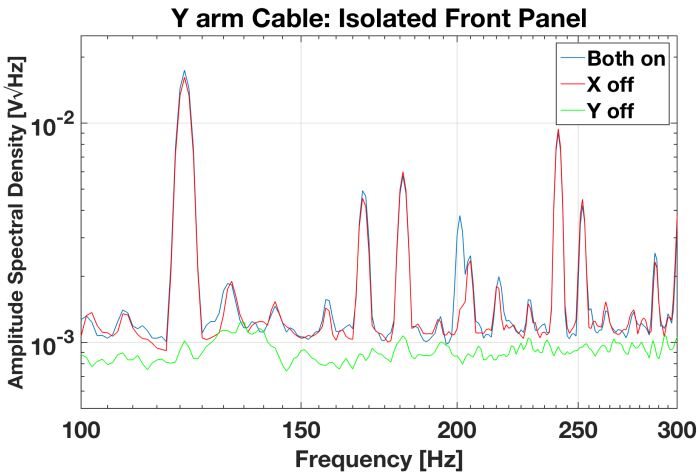

(a) Y arm cable data using conductive front panel (b) Y arm cable data using isolated front panel

Figure 16: Comparison between the isolated X (a) and the isolated Y(b)

tested in the real system.

After getting no conclusive results from the test setup, the box was moved into the real system. There, the ALS Beatbox is more isolated, leaving less potential for noise entering there. I tested the real system three ways, and drove a frequency of 30.019 Hz through the X Arm and a frequency of 30.019203 Hz through the Y Arm, giving a difference of 203 Hz. First, I took measurements with the old, shorter cables in an un-isolated styrofoam box. I then took measurements with both the isolated and conductive panels on the box I built to hold the new, longer cables. After multiplying the ASDs with the new, longer cables by a factor of 0.6 to create an even comparison between the old and new setup, it can be seen in Figure 17 that using the box with the conductive panel reduced the noise at 203 Hz by a factor of more than 3. The isolated panel made the crosstalk worse, indicating that the isolated panel most likely ruined the Faraday cage that the box I built provides with the conductive panel. Therefore, the 40m Interferometer is currently using the electrically

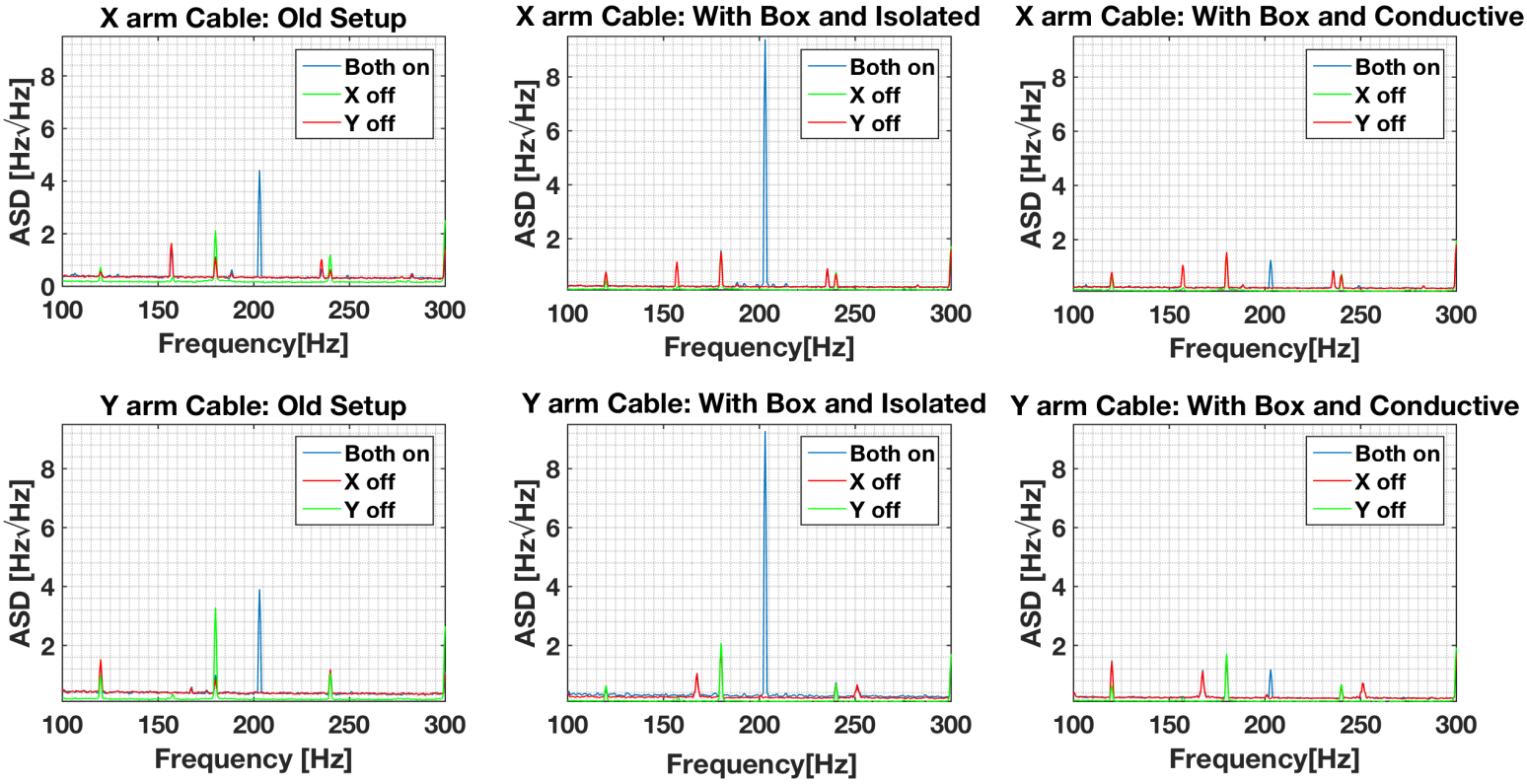

Figure 17: Real-System testing of the two panels with the box and the cables without the box

isolated box with the conductive panel to hold cables for the ALS Delay Line.

References

[1] G. Cella and A Giazotto *Interferometric Gravity Wave Detectors*. Review of Scientific Instruments 82, 101 101 (2011).

[2] John Bechhoefer, *Feedback for Physicists: A Tutorial Essay on Control*. Review of Modern Physics, Volume 77 (July 2005).

[3] J. Driggers, M. Evans, K. Pepper, and R. Adhikari, *Active Noise Cancellation in a Suspended Interferometer*. arxiv:1112.2224. (December 2011).

[4] R. DeRosa, J. Driggers, D. Atkinson, H. Miao, V. Frolov, M. Landry, J. Giaime, and R. Adhikari, *Global Feed-forward Vibration Isolation in a km scale Interferometer*. Quantum Grav. 29 215008 (2012).

[5] Natanael Fontes *An Analysis of the IIR and FIR Wiener Filters with Applications to Underwater Acoustics*. Naval Postgraduate School (1997).

[6] *Introduction to Piezoelectric Accelerometers* PCB Piezotronics (2015).

[7] M.J. Usher, C. Guralp, and R.F. Burch. *The Design of Miniature Wideband Seismometers* Geophysical Journal of the Royal Astronomical Society (1978).

[8] S. Orfanidids *Introduction to Signal Processing* Pearson Education Inc., 2010.

[9] J. Gray and D. Allan. *A Method for Estimating the Frequency Stability of an Individual Oscillator* National Institute of Science and Technology.

[10] J. Driggers *Noise Cancellation for Gravitational Wave Detectors* California Institute of Technology (2015).

[11] R. Daniels *Approximation Methods for Electronic Filter Design* Bell Telephone Laboratories, 1974.

[12] S. Smith *The Scientist and Engineer's Guide to Digital Signal Processing* California Technical Publishing (1997).

[13] http://www.mathworks.com/help/dsp/ref/fdesign.bandpass.html

[14] https://www.sintef.no/projectweb/vectfit/passivity/

[15] B. Widrow and S. Stearns *Adaptive Signal Processing* Prentice-Hall Inc., 1985.